On the Use of Tuned Mass Dampers for Reducing the Nonlinear Vibrations of Planar Parallel Cable Robots

Diego A. Zamora-García, Alejandro C. Ramirez-Reivich, and Ma. Pilar Corona-Lira
National Autonomous University of Mexico/School of engineering, Mexico City, Mexico
Email: diego77@comunidad.unam.mx; areivich@unam.mx; pilicorona@comunidad.unam.mx

Jonathan Eden and Denny Oetomo
The University of Melbourne/Melbourne School of Engineering, Melbourne, Australia
Email: jpeden@student.unimelb.edu.au; doetomo@unimelb.edu.au

***Abstract*— The out of plane free vibrations of planar parallel cable robots possess a long duration, this is a problem for applications that require a fast settling time, which corresponds to the time necessary for the vibration to stop. We evaluated the effectiveness of a tuned mass damper (TMD) as a solution to minimize the settling time of these nonlinear vibrations. This paper presents a dynamical model of a two degree of freedom nonlinear mechanical system. Using this model, a numerical search was conducted to identify the optimal set of design parameters. During our investigations, it was observed that with an optimized tuned mass damper reductions of 96.51% of the settling time in the best case can be achieved and that the effectiveness of this optimized TMD is relatively homogeneous in the workspace with the exception of the workspace corners.**

***Index Terms*—Cable robots, Tuned mass damper, nonlinear vibrations, Optimization.**

I. Introduction

Cable-driven parallel robots henceforth referred to as CDPRs, are a relatively new type of robotic manipulator in which wired transmission is used in place of rigid links. One end of each cable is attached to an actuator, and the other end is attached to an end effector and through the coordinated extension and retraction of the cables, the position of the end effector can be controlled [1], [2] and [3]. CDPRs possess a number of advantages including simple structure, lightweight, small inertia, fast response, high-speed performance and large operating workspace. With these advantages, CDPRs have been applied to a wide range of applications including the control of radio telescopes [4], biomechanical modeling rehabilitation [5] and [6], and high-speed manufacturing [7].

Due to their low stiffness and flexible actuating cables, the use of CDPRs is often limited by the effect of vibration. Kawamura et al. first experimentally studied the effects of the nonlinear elasticity of high-speed cable robots [8]. The particular problem of vibration for hardware in the loop cable robot simulation was further studied by Ma and Diao [9]. Tang et al. [10] found through numerical simulations that the mass and eccentricity of the end effector contribute to instability.

In the specific case of planar parallel cable robots, Diao and Ma [11] found that the transversal vibration of the wire in their line of equilibrium represented only the 1.4% of the total vibration in the end effector. The deflection caused for a force applied normal to the working plane was also further studied by Smith et al. [12] in which it was observed that the CDPR deflection differs throughout the workspace and that the oscillation frequencies are in general within the range of 0.5 - 1 Hz. These specific out of plane vibrations possess a long settling time and therefore subsequently bring undesirable consequences to applications that require a fast operation.

To address the vibrations that occur in CDPR operation, the use of pretension has been proposed [8] and [12]. This solution, however, possesses some disadvantages including increased energy consumption, increased actuator torque requirements and a reduction of the load capacity of the robot. These disadvantages have an impact on the manufacturing cost, where there is the necessity of bigger actuators, and in the operation costs, where the robot needs more energy.

Due to the lack of actuation orthogonal to the work plane, out of plane vibrations for planar CDPRs represent the most common form of CDPR vibration. Specifically, when the end effector is in a static position of the workspace, perturbation of the end effector results in out of plane vibrations. These vibrations usually have a long settling time and therefore limit the effectiveness of the CDPRs in applications that require a quick settling time.

One possible option to attenuate the out of plane vibrations of CDPR end effectors is the implementation of a damper. However, such a damper must not be connected to the mechanical ground since for planar CDPRs the end effector moves throughout the workspace. As a result, a floating damper is needed, where one candidate is the use of a tuned mass damper, referred

Manuscript received March 31 2018; revised April 15, 2019.

doi: 10.18178/ijmerr.8.3.406-412

from now on as TMD. The linear TMD is a well-studied option to mitigate vibrations in structures [13], [14] and [15]. Typically parameters of a TMD are optimized to minimize the magnitude of the vibration over a range of specified frequencies. For planar CDPRs, however, it is necessary to optimize the parameters in the time domain to minimize the settling time of the vibration after an end effector perturbation.

In this paper, the performance of a tuned mass damper as a potential solution of the out of plane vibrations of planar CDPRs is investigated. The focus of this study is the mitigation of vibration from positions of the static equilibrium. This is evaluated throughout the CDPR workspace where it is shown that the use of a TMD results in a substantial reduction of out of plane vibrations.

The remainder of this paper is organized as follows: Section II describes the configuration of the studied cable robot and provides a derivation of the dynamical model for this class of robot. The algorithms used for the optimization procedure and the evaluation of the behavior of the TMD in the workspace of the planar CDPR is presented in Section III. Section IV presents the results of the optimization algorithm applied to the case study CDPR. Finally, the discussion and the pertinent conclusions are provided in Section V.

II. The Mathematical Model

In the case of a planar CDPR with one rigid end effector, the principal vibration is in the out of plane direction. This is because the restoration force resulting from the cable elasticity is higher in the cable's axial direction than in the transversal directions of the work plane [16]. These vibrations have a larger amplitude and duration compared with the vibrations in the other five degrees of freedom [12]. In this paper, the study of a case study four cables planar CDPR is considered. For illustrative purposes, the explanation of the mathematical model will be made using two cables and one mass case. The model is subsequently extended through the superposition of additional cable dependent terms in the model.

A. The Configuration of the Planar CDPR

Fig. 1 depicts the planar CDPR that is used throughout this study. This CDPR is actuated by four cables attached to the corners of the 1m by 1m frame and the 0.1m by 0.1m end effector. As shown in the figure, the working plane is $x_f - y_f$and is denoted by h_f. As a result, z_f is the direction of the out of plane vibrations of the end effector, where there is no restriction.

In this study, the out of plane vibrations that happen when the end effector is in a static position in the working plane are considered. This means that the vibrations occur in the z_f direction when the end effector is not moving in the work space. This vibration could be caused by momentary external disturbances or misalignments in the mechanical assembly.

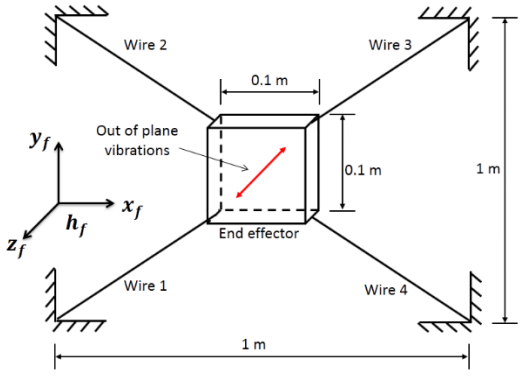

Figure 1. Cable driven parallel robot configuration.

B. The Modeling of the Out of Plane Vibrations

The cables are modeled as a spring and damper in parallel with negligible mass. This is consistent with the approach of [17] and the resulting cable model is illustrated in Fig. 2. The cable presents not only axial vibrations but also present transversal vibrations to their line of equilibrium. However, it has been demonstrated analytically that these transversal vibrations represent only the 1.4% of the vibration of the end effector [11] and therefore the transversal vibration is neglected from this analysis. The values of the spring constant and the coefficient of viscous friction for each cable are represented as k_{cn} and b_{cn}, respectively, where these values vary as a function of the cable lengths. The rigidity of the cable in the axial direction decreases with the increase of the length of the cable, while the energy dissipation of the cable increases with the increase of the cable length. A linear relation between these parameters and the length of the cable us assumed such that k_{cn} and $b_{cn}$are given by

$$k_{cn} = c_1 l_{on} + c_2, \quad (1)$$

$$b_{cn} = c_4 l_{on} + c_4, \quad (2)$$

where C_1, C_2, C_3 and C_4 are modeling constants and l_{on} is the length of the cables in their steady state.

A simple cable robot with two cables and one end effector is now presented to explain the model of the out of plane vibrations. There is a fixed reference h_f in which the displacement of the end effector is in the x_f direction through the coordinated changes in the lengthsl_{on}. The k_{cn} and b_{cn} are parameters of stiffness and damping as previously explained, and the end effector is represented as a massm_e. The magnitude l_n is the length of the cables in each instant time.

Fig. 3 shows the same system in a perturbed state induced by a force $F = f(t)$ in the z_f direction. There is a displacement z_1 induced by the force. Due to this force, the springs and dampers present an elongation and a rotation resulting in a geometrically induced nonlinear behavior. This results in new values of L_n. In this case study, the force $F = f(t)$ is an impulse force. This will result in an oscillatory movement of the end effector in the z_f direction. These free vibrations represent the geometrically nonlinear out of plane vibrations.

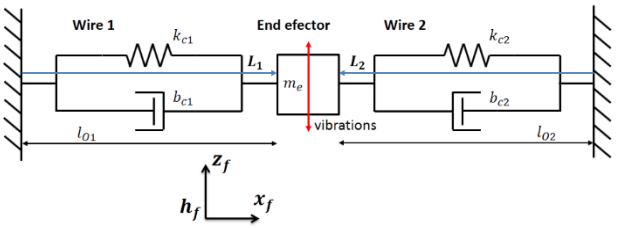

Figure 2. Simplified cable robot consisting of two cables and one end effector.

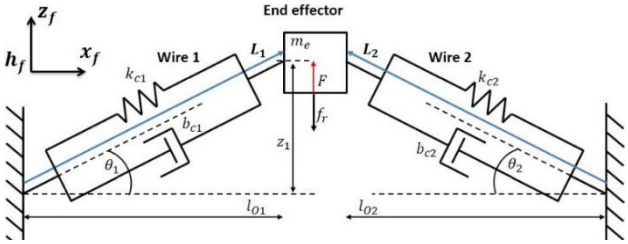

Figure 3. The simplified CDPR system in a perturbed state.

These are geometrical because the elements are linear but their response is nonlinear due to their geometric displacement.

The total cable force consists of two elements: the spring force f_{ckn} and the damper force f_{cbn}. Each of these elements varies as a function of the displacement in z_f direction. In the case of the force of the spring, the pretension f_{ptn} must also be considered. Noting that the spring force f_{ckn} is a linearly dependent function of z_f it can therefore be seen that

$$f_{ckn} = (f_{rn} + f_{ptn})sin(\theta_n). \quad (3)$$

Where the force of the spring due its elongation is described by

$$f_{rn} = k_{cn}(L_n - l_{on}). \quad (4)$$

The elongation and contraction of the spring as a function of the z_f displacement is described by

$$L_n = \sqrt{{l_{on}}^2 + z^2}. \quad (5)$$

The angle θ_n of the cable with respect to the equilibrium as a function of the z_f displacement is described by.

$$\theta_n = tan^{-1}(z/l_{on}). \quad (6)$$

Replacing (4), (5) and (6) in (3) it can be seen that the geometrically nonlinear behavior of the spring is given by

$$f_{ckn} = (k_{cn}\left(\sqrt{{l_{on}}^2 + z^2} - l_{on}\right) + f_{ptn})Sin(\tan^{-1}(z/l_{on})). \quad (7)$$

In the case of the geometrically nonlinear damping, a given model is showed in [18] and [19] as

$$f_{cbn} = b_{cn}\left(\frac{z^2}{{l_n}^2+z^2}\right)\frac{dz}{dx}. \quad (8)$$

Taking into account that the lengths of the cables are changing all the time due to their axial elasticity, it can be seen that

$$l_n = \sqrt{{l_{on}}^2 + z^2}. \quad (9)$$

As a result, the final equation of the force in the z_f direction due to the dampers is a function of the velocity and the position is

$$f_{cbn} = b_{cn}\left(\frac{z^2}{{l_{on}}^2+2z^2}\right)\frac{dz}{dx}. \quad (10)$$

Finally, the friction with the air as a force f_r, which is a function of the velocity of the end effector in the z_f direction is given by

$$f_r = b_r\left(\frac{dz_1}{dt}\right). \quad (11)$$

where b_r is the viscous friction coefficient.

With the equations of the forces in the z_f direction due to the springs and dampers, a dynamical model of one degree of freedom including the four cables can be constructed as

$$m_e\frac{d^2z}{dt^2} + F_{rz} + F_{bz} + f_r = f(t), \quad (12)$$

in which F_{rz} and F_{bz} are composed of four terms each one, related to each cable of the robot configuration. F_{rz} is composed of the sum of the spring force (7) for each cable such that

$$F_{rz} = f_{ck1} + f_{ck2} + f_{ck3} + f_{ck4}. \quad (13)$$

Similarly, the term F_{bz} is composed of the sum of the spring force (10) for each cable such that

$$F_{bz} = f_{cb1} + f_{cb2} + f_{cb3} + f_{cb4}. \quad (14)$$

C. The Integration of a Tuned Mass Damper

The most common representation of a linear TMD consists of a two degree of freedom spring-mass-damper model. The diagram is presented in Fig. 4. The m_e, k_e and b_e represent the mass, stiffness and damping parameters of the structure, respectively, and the m_a, k_a and b_a are the equivalent parameters of the damper. The objective is to tune in the last three parameters in order to minimize the settling time of the free vibration of the coordinate x_1.

The mathematical model that defines the dynamics of this system is the set of two differential equations

$$m_e\frac{d^2x_1}{dt^2} + (b_1 + b_2)\frac{dx_1}{dt} + (k_1 + k_2)x_1 - b_2\frac{dx_2}{dt} - k_2x_2 = 0. \quad (15)$$

$$m_a\frac{d^2x_2}{dt^2} + b_2\frac{dx_2}{dt} + k_2x_2 - b_2\frac{dx_1}{dt} - k_2x_1 = 0. \quad (16)$$

Fig. 5 shows the implementation of a linear TMD in the previously explained geometrically nonlinear system. The model must now consist of two degrees of freedom, where the additional degree of freedom is denoted z_2.

The final model is then given by the integration of the TMD dynamics (15) and (16) with the total force terms (13) and (14). This results in the system dynamics shown in equations (17) y (18).

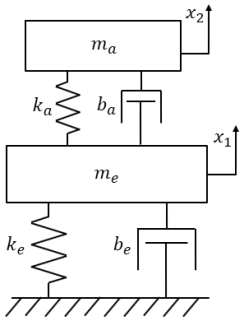

Figure 4. Scheme of a linear TMD.

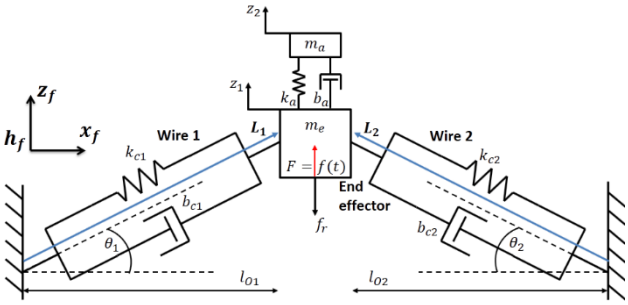

Figure 5. The implementation of a tuned mass damper in the out of plane vibrations.

$$m_e \frac{d^2 z1}{dt^2} + F_{rz} + F_{bz} + b_a \frac{dz1}{dt} - b_a \frac{dz2}{dt} + k_a z_1 - k_a z_2 = f(t). \quad (17)$$

$$m_a \frac{d^2 z_2}{dt^2} + b_a \frac{dz_2}{dt} - b_a \frac{dz_1}{dt} + k_a z_2 - k_a z_1. \quad (18)$$

Fig. 6 depicts the spring force in the z_f direction as a function of the displacement of the end effector in thez_f direction for different values of k_{cn}, while Fig. 7 displays the damping forces in the z_f direction due to a damper as a function of the displacement of the end effector in the z_f direction for different velocities of the displacement. From the graphs, two interesting points can be observed. First, the graphs displays geometrically induced nonlinearities. Second, there is a zone of low stiffness and low damping near the equilibrium point, this is the cause of the small amplitude and low duration free vibrations in the z_f direction of the end effector after a perturbation.

III. The Procedure for the Numerical Simulations

Computational numeric methods were used to do the optimizations and simulations. This made use of the software Matlab® version R2013a to schedule scripts which call functions of the dynamic models. The dynamical models are solved with the ode45 function of Matlab®.

The goal for the optimization is to find the values of m_a and k_a for the tuned mass damper in the four cable one end effector case presented in Section II. The b_a is not a usual parameter to optimize, this should be first determined experimentally from the mechanical assemble and then established in the model for the optimization procedure.

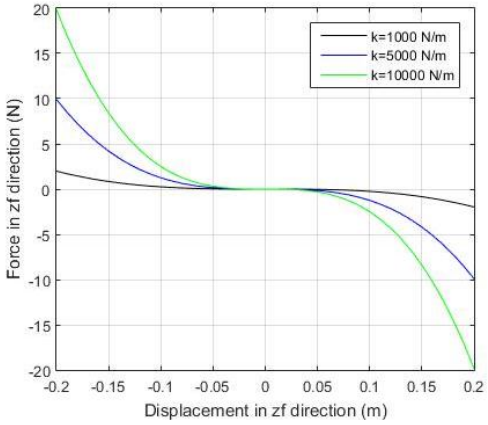

Figure 6. The force in the zf direction due to the springs.

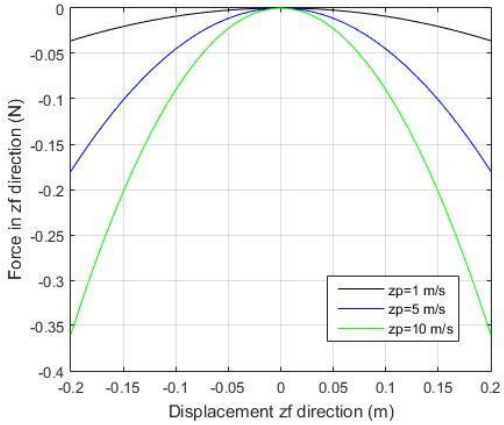

Figure 7. The force in zf direction due to the dampers.

This optimization was made in the center of the workspace of the CDPR with the objective to minimize the settling time of the vibrations inz_1, the coordinate of the end effector. A calculation of the lengths of the cables is made using the CDPR inverse kinematics. To calculate the values of the k_{cn} and b_{cn}, (1) and (2) are used as explained in the previous section. Finally, to determine the values c_1, c_2, c_3 and c_4 two hypothetical points are used for each parameter, $p1 = (0.05,30000)$ and $p2 = (1,5000)$ in the case of the parameter k_{cn}, $p1 = (0.05,0.2)$ and $p2 = (1,1)$ in the case of the b_{cn} parameter. The final value of the parameters is showed in table 1.

TABLE I. Parameters For The Model Of Four Cables And One End Effector

Parameter	Value
m_e	1 Kg
pt	50 N
k_{c1} to k_{c4}	12840 N/m
b_{c1} to b_{c4}	0.7148 N s/m
l_{o1} to l_{o4}	0.6364 m

The algorithm for the optimization uses a sweep parameter methodology, two "for" cycles sweep the parameters for the desired range of mass values m_a and a desired range of stiffness values k_a. In each iteration, the settling time is computed and saved in a matrix, finally, these values are plotted in a 3D surface to locate the lowest value of the settling time and the corresponding optimized values of m_a and k_a. For the optimization a mass range of 0.05 Kg to 0.15 Kg was used with a resolution of 3 g and a stiffness range of 1 N/m to 15 N/m with a resolution of 0.4 N/m.

For (Minimum m_a to Maximum m_a)
  For (Minimum k_a to Maximum k_a)
    Run the simulation
    Get the settling time
    Save the settling time in a matrix
  end
end
Graph surface

Figure 8. Algorithm for the optimization of the tuned mass damper.

The data of this optimization were analyzed evaluating the percentage of reduction of the settling time, and the mass ratio.

Through numerical simulations, the behavior of the system without a tuned mass damper and with an optimized tuned mass damper are compared in different points of the workspace. A map of the percentage of attenuation of the vibration in different points of the workspace can, therefore, be constructed, from which different regions of the effectiveness of the optimized tuned mass damper can be identified.

For the given case study, this analysis only uses the IV quadrant of the workspace due to the symmetric distribution of the cables. In this IV quadrant, 625 points to evaluate the settling time without TMD and the settling time with the optimized TMD were used. Using this data a calculation of the percentage of reduction can be conducted in each one of the 625 points.

The algorithm used for the evaluation of the tuned mass damper in the work space is given below

For (first point – last point)
  Get the parameters of the cable with inverse cinematic
  Run a simulation without TMD
  Get the settling time.
  Save the settling time in a matrix 1
  Run a simulation with TMD
  Get the settling time.
  Save the settling time in a matrix 2
End
Compute the percentage of reduction in each point
Graphic Matrix 1 (Settling time without TMD)
Graphic Matrix 2 (Settling time with TMD)
Graphic percentage of reduction.

Figure 9. Algorithm for the evaluation of the tuned mass damper in the IV quadrant of the workspace.

IV. Results

In this section, the application of an optimized TMD is illustrated in the case study planar four cable planar CDPR. The effectiveness of the TMD is evaluated firstly at a single pose before being subsequently evaluated over the complete CDPR workspace.

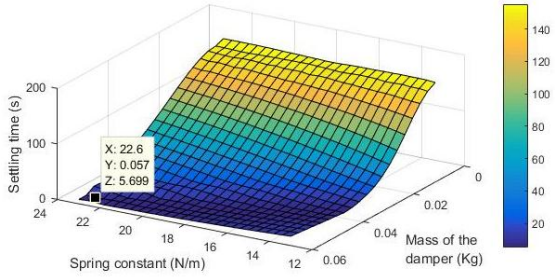

Figure 10. Settling time of the TMD for different spring stiffness and damping values.

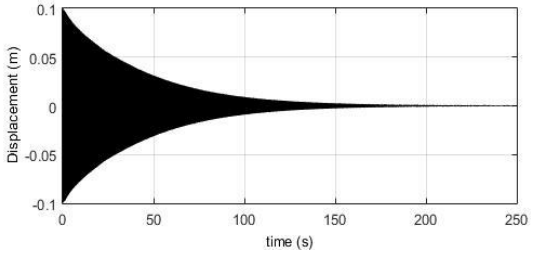

Figure 11. Time response of free vibration of the end effector along the zf direction without the optimized tuned mass damper.

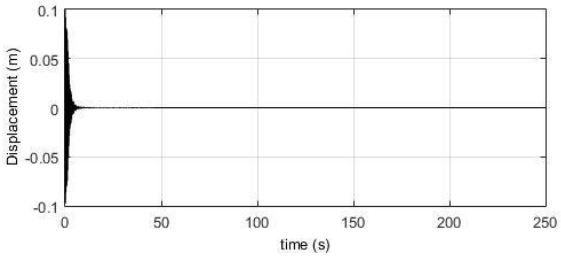

Figure 12. Time response of a free vibration of the end effector along the zf direction with the optimized tuned mass damper.

A. The Effectiveness of a TMD in the Nonlinear Vibrations.

Fig. 10 shows the results of the sweep process, where the settling time is plotted as a surface on the k_a and m_a axes. The optimal values were found as $m_a = 0.057Kg$ and $k_a = 22.6\,N/m$, respecitvely, in which these parameters achieved a settling time of $5.699s$ and a mass ratio of 0.057.

Fig. 11 depicts the time response without the TMD. It can be seen that without the TMD the system possesses settling time of $162.66s$. In contrast, Fig. 12 shows the time response with the TMD in which the resulting settling time is found to be $5.69s$. This represent a reduction of 96.51 % of the settling with the use of an optimized TMD in the center of the work space.

B. The Effectiveness of a TMD in the CDPR Work Space

The effectiveness of the optimized TMD in all the workspace can be evaluated by looking at Fig. 13. This figure shows the value of the settling time over 625

distinct points located throughout quadrant IV of the workspace.

Fig. 14 represents the settling time in 625 places of the workspace with the use of the optimized TMD. It can be seen that the use of the optimized TMD results in a significant reduction of the settling time over most of the workspace. This is further visualized through the use of Fig. 15, which represents the percentage of reduction in the IV quadrant of the workspace.

V. Discussion and Conclusions

In this work, the effectiveness of a TMD as a solution for the out of plane vibrations in planar CDPRs has been evaluated. The vibration of the robot in the out of plane direction was modeled and it was found that there are geometrically induced nonlinearities. To attenuate these nonlinearities a TMD was introduced into the model and optimized in order to reduce the settling time of the out of plane vibrations. Finally, through numerical simulations, we evaluated the behavior of the optimized TMD in different points of the workspace.

It was found that the use of a TMD can significantly reduce the settling time of out of plane vibrations induced by an impulse force in the end effector. In the center of the workspace, where the TMD was optimized, there is a reduction of 96.51%. This significant reduction is consistently observed throughout the workspace with the exception of the workspace corners. This is likely because in the corners the shorter cable presents a high rigidity. Since CDPRs are typically operated away from the workspace boundary, the effects of this smaller reduction are likely to be minimal.

The required TMD mass ratio was observed to be quite low. As a result, it is unlikely that the load capacity of the robot will be significantly affected. However, It should be noted that due to the small dimensions required, there could be some challenges in the fabrication of a suitable TMD for real-world applications.

Future work will investigate the implementation of an electromagnetic tuned mass damper, to harvest energy instead of dissipating it. Additionally, the results of this theoretical study will be evaluated on an experimental prototype.

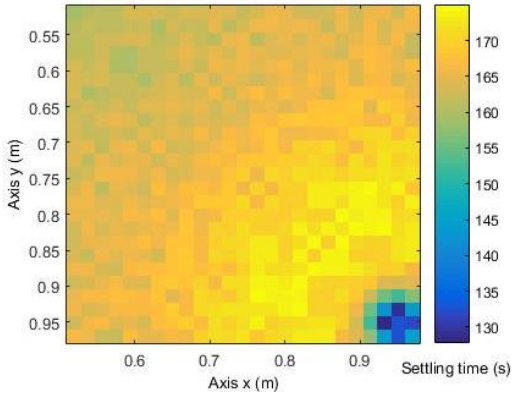

Figure 13. Settling time in different points of the workspace of the IV quadrant without a TMD.

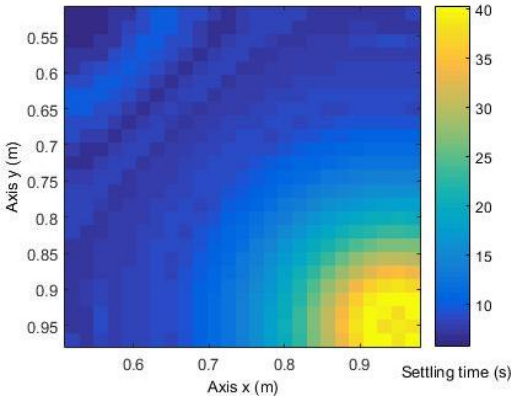

Figure 14. Settling time in different points of the workspace of the IV quadrant with an optimized TMD.

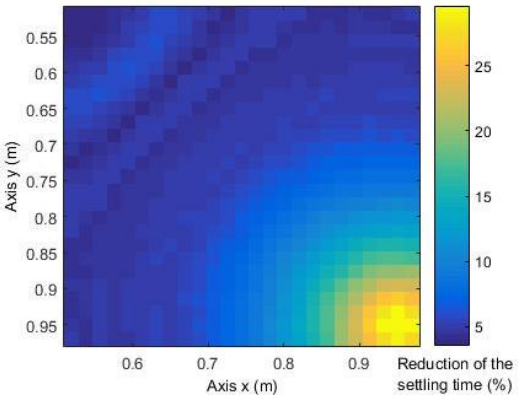

Figure 15. Graph of the percentage of reduction of the settling time in different points of the workspace.

Acknowledgment

The authors would like to recognize the support of the PAPIIT UNAM no. 102318 with the name “Investigación y análisis de la influencia del efecto de amortiguamiento electromagnético en la atenuación de vibraciones en sistemas actuados por tensores” and the support of the Australian Government through the Department of Education and Training and the Australian Academy of Science.

References

[1] M. Hiller, S. Fang, S. Mielczarek, R. Verhoeven, and D. Franitza, “Design, analysis and realization of tendon-based parallel manipulators,” *Mechanism and Machine Theory*, vol. 40, pp. 429-445, 2005.

[2] D. Lau, D. Oetomo and S. K. Halgamuge, “Generalized modeling of multilink cable-driven manipulators with arbitrary routing using the cable-routing matrix,” *IEEE Transactions on Robotics*, vol. 29, no. 5, pp. 1102-1113, 2013.

[3] D. Lau, D. Oetomo, and S. K. Halgamuge, “Inverse dynamics of multilink cable-driven manipulators with the consideration of Joint interaction Forces and moments,” *IEEE Transactions on Robotics*, vol. 31, n º2, pp. 479-488, 2015.

[4] B. Zi, B. Duan, J. Du, and H. Bao, “Dynamic modeling and active control of a cable-suspended parallel robot,” *Mechatronics*, vol. 18, n º1, pp. 1-12, 2008.

[5] Y. Mao and S. K. Agrawal, “Design of a cable-driven arm exoskeleton (CAREX) for neural rehabilitation,” *Transactions on Robotics*, vol. 28, n º4, pp. 922-931, 2012.

[6] D. Lau, J. Eden, D. Oetomo and S. K. Halgamuge, "Musculoskeletal static workspace analysis of the human shoulder as a cable-driven robot," *IEEE/ASME Transactions on Mechatronics*, vol. 20, n º2, pp. 978-984, 2015.

[7] A. Pott, H. Mütherich, W. Kraus, V. Schmidt, P. Miermeister and A. Verl, "IPAnema: A family of Cable-Driven Parallel Robots for Industrial Applications," in *Mechanisms and Machine Science*, Heidelberg New York Dordrecht London, Springer, 2013, pp. 119-134.

[8] S. Kawamura, W. Choe, S. Tanaka and S. R. Pandian, "Development of an ultrahigh speed robot FALCON using wire drive system," in *IEEE International Conference on Robotics and Automation*, Nagoya, Japan, 1995.

[9] O. Ma and X. Diao, "Dynamics analysis of a cable-driven parallel manipulator for hardware-in-the-loop dynamic simulation," in *International Conference on Advanced Intelligent Mechatronics*, Monterey, California, USA, 2005.

[10] A. Tang, Y. Li, L. Kong and X. Cheng, "Vibration analysis of tendon-based parallel robot for processing," *Advanced Materials Research*, Vol. 1, pp. 1086-1091, 2013.

[11] D. Xiumin and O. Ma, "Vibration analysis of cable-driven parallel manipulators," *Multibody System Dynamics*, vol. 21, no. 4, pp. 347-360, 2009.

[12] V. Schmidt, W. Kraus and A. Pott, "Presentation of experimental results on stability of a 3 dof 4-cable-driven parallel robot without constraints," in *Second International Conference on Cable-Driven Parallel Robots*, Duisburg, Alemania, 2014.

[13] R. Villalverde, "Reduction in seismic response with heavily-damped vibration absorbers," *Earthquake Engineering and Structural Dynamics*, vol. 13, pp. 33-42, 1985.

[14] F. Sadek, B. Mohraz, A. W. Taylor and R. M. Chung, "A method of estimating the parameters of tuned mass dampers for seismic applications," *Earthquake Engineering and Structural Dynamics*, vol. 26, n º6, pp. 617-635, 1997.

[15] G. Bekdas and S. M. Nigdeli, "Estimating optimum parameters of tuned mass dampers using harmony search," *Engineering Structures*, vol. 33, no. 9, pp. 2716-2723, 2011.

[16] S. Kawamura, H. Kino, and C. Won, "High-speed manipulation by using parallel wire-driven robots," *Robotica*, vol. 18, n º1, pp. 13-21, 2000.

[17] Y. B. Bedoustani, H. D. Taghirad and M. M. Aref, "Dynamics analysis of a redundant parallel manipulator driven by elastic cables," in *International Conference on Control, Automation, Robotics and Vision*, Hanoi, 2008.

[18] B. Tang and M. Brennan, "A comparison of two nonlinear damping mechanisms in a vibration isolator," *Journal of Sound and Vibration*, vol. 332, n º3, pp. 510-520, 2013.

[19] J. C. Carranza, M. J. Brennan and B. Tang, "Sources and propagation of nonlinearity in a vibration isolator nonlinearity in a vibration isolator damping," *Journal of Vibration and Acoustics*, vol. 138, no. 2, 2015.

Diego A. Zamora-Garcia was born in Córdoba city, Mexico, on January 15th of 1990. He received the B.Eng. degree from the state university of Veracruz in 2012 and the Master in Engineering from the National Autonomous University of Mexico in 2015, he is currently a Ph.D. candidate (mechanical engineering) from the National Autonomous University of Mexico.

He had participated in different projects of research and development at the center of advanced engineering at the National Autonomous University of Mexico. He is interested in mechatronic design and automation.

Alejandro C. Ramirez-Reivich was born in Mexico City, Mexico. He received the B.Eng. from the National Autonomous University of Mexico in 1983 and the Master in Engineering degree from the same institution in 1986. He received the Ph.D. degree at Lancaster University in the United Kingdom in 1995.

He had the opportunity to design new products together with graduate and ungraduated students. The integration and development of new manufacturing processes, and make new systems for Mexican and foreign companies.

Ma. Del Pilar Corona-Lira was born in Mexico City, Mexico. She received the B.Eng. from the National Autonomous University of Mexico in 1992 and the Master of Science at Lancaster University in the United Kingdom in 1995. She received a Ph.D. from the National Autonomous University of Mexico in 2013.

She had developed new products integrating graduate and ungraduated students in its process. She has collaborated on several projects that involved multidisciplinary teams. She has taught different courses on electronics and mechatronics. She is interested in instrumentation, signal processing and surface inspection by Image processing.

Jonathan Eden received his B.Sc. And M.End at the University of Melbourne in 2011 and 2013, respectively. He began his Ph.D. at the University of Melbourne in 2014. He is currently a postdoctoral fellow at Imperial College, London. His research interests include the analysis and control of constrained and redundantly actuated robotic systems and the kinematic and dynamic analysis of cable-driven parallel manipulators.

Denny Oetomo received B.Eng (Hons 1, Australian National University, 1997) and Ph.D. in robotics (National University of Singapore, 2004).

He was a Research Fellow at Monash University, (2004–2006) and at INRIA Sophia-Antipolis (COPRIN), France (2006–2007). He joined the Department of Mechanical Engineering, The University of Melbourne, in January 2008, where he is currently an Associate Professor. His research interests include the area of kinematics, dynamics, and the effective control strategies of complex mechanisms; applied to clinical, assistive robotics.

